

Bottomonium states versus recent experimental observations in the QCD-inspired potential model^{*}

Tian Wei-Zhao^{1,2} CAO Lu¹ YANG You-Chang² CHEN Hong^{1;1)}

¹School of Physical Science and Technology, Southwest University, Chongqing 400715, China

²Department of Physics, Zunyi Normal College, Zunyi 563002, China

Abstract: In the QCD-inspired potential model where the quark-antiquark interaction consists of the usual one-gluon-exchange and the mixture of long-range scalar and vector linear confining potentials with the lowest order relativistic correction, we investigate the mass spectra and electromagnetic processes of a bottomonium system by using the Gaussian expansion method. It reveals that the vector component of the mixing confinement is anticonfining and takes around 18.51% of the confining potential. Combining the new experimental data released by Belle, BaBar and LHC, we systematically discuss the energy levels of the bottomonium states and make the predictions of the electromagnetic decays for further experiments.

Key words: bottomonium, quark potential model, mass spectroscopy, Gaussian expansion method

PACS: 14.40.Nd, 12.39.Jh, 13.40.Hq

1 Introduction

With the increasing observations of the bottomonium ($b\bar{b}$) states and bottomonium-like resonances[1], it is worth revisiting the $b\bar{b}$ states to identify the possible candidates. Very recently, the $\eta_b(2S)$ was firstly observed in the $\Upsilon(2S)$ radiative decays at a $\sim 5\sigma$ level [2] at a mass of $9974.6 \pm 2.3(stat) \pm 2.1(syst)$ MeV and corresponds to the $\Upsilon(2S)$ hyperfine split of $48.7 \pm 2.3(stat) \pm 2.1(syst)$ MeV. Also as the first observation, the $h_b(1P)$, $h_b(2P)$ [3] and $\chi_b(3P)$ multiplets[4] have been found recently. Including the $\Upsilon(10860)$ [5, 6] and $\Upsilon(11020)$ [7, 8], the bottomonium-like states have aroused lasting interest in theoretical investigations [9, 10] since their establishment.

The $b\bar{b}$ spectroscopy is considered an excellent laboratory to examine the quark-antiquark potential within the non-relativistic framework due to the large b -quark mass. The QCD inspired potential models have played an important role in investigating the spectra for both charmonium and bottomonium [11, 12]. The long-range confinement is one of the essential ingredients in most quark potential models. However, the nature of the confining mechanism is still far away from clear. In the original Cornell model [13, 14], it was assumed to be a Lorentz scalar, which gives a vanishing long-range magnetic contribution and agrees with the flux tube picture of quark confinement [15]. Another possibility is that the confinement may be a more complicated mixture of scalars and time-like vectors, while the vector potential is anticon-

fining [16, 17]. It has been indicated that the calculated results of electroweak decay rates for heavy mesons with a pure scalar confinement are in worse agreement with data than adopting a vector potential [18–20].

Besides the potential model, the numerical method is very important for calculating the decays and spectrum of the bound states system. As several numerical methods fail in the potentials with the higher than the second orders in $1/r$, the $\mathcal{O}(v^2/c^2)$ corrections to the quark-antiquark potential usually have to be treated as mass shifts using the leading-order perturbation theory [9, 17, 21]. Therefore, both perturbation and nonperturbative treatments have been taken into account recently in Ref. [22], which indicates the most significant effect of different treatments on the wave functions. The nonperturbative treatment brings each state with its own wave function, while the perturbative treatment leads to the same angular momentum multiplets sharing the identical wave function. It is known that the radiative transitions, leptonic and double-photon decay widths are quite sensitive to the shape of wave function and its information at the origin. Exactly, each physical particle owning a different quantum number should behave with a distinguishing state wave function.

We have performed such a nonperturbative treatment on the potential model calculations for charmonium system in Ref. [23] and compared the different confining assumptions. Fitting with the well-established charmonium states, the Lorentz vector component parameter is

Received 14 March 2009

^{*} Supported by National Natural Science Foundation of China (11175146, 11047023 and 11265017) and the Fundamental Research Funds for the Central Universities (XDJK2012D005)

1) E-mail: chen@swu.edu.cn

expected to be 22%, which implies about one-fifth vector exchange in the $c\bar{c}$ interquark confining potential. The subtleness of the obtained wave functions has been examined via the electromagnetic transition, leptonic decay and two-photon width. Our predictions for the charmonium are in reasonable agreement with experiments. It would be interesting and rewarding to extend the current framework to the bottomonium states in this paper.

In the next section we briefly introduce the QCD-inspired quark model and the variational approach adopted in this work. Following with the numerical results, we discuss the latest experimental observations in Section 3. Finally, a summary is presented in Section 4.

2 Potential model and calculational approach

We begin with the nonrelativistic potential model, where the linear confinement has been assumed as Lorentz scalar-vector mixture [16, 17],

$$V_S = \beta(1 - \varepsilon)r, \quad V_V = -\frac{4}{3}\frac{\alpha_s}{r} + \varepsilon\beta r, \quad (1)$$

where ε stands for the vector exchange scale. Then the spin-spin, spin-orbit and tensor interactions can be directly derived from the standard Breit-Fermi expression to order (v^2/c^2) with the quark mass m_b . Explicitly, the adopted $b\bar{b}$ potential is [23]

$$\begin{aligned} V_{b\bar{b}} = & -\frac{4}{3}\frac{\alpha_s}{r} + \beta r + \frac{32\pi\alpha_s}{9m_b^2}\tilde{\delta}_\sigma(r)\mathbf{S}_b \cdot \mathbf{S}_{\bar{b}} \\ & + \left[\frac{2\alpha_s}{m_b^2 r^3} + \frac{(4\varepsilon - 1)\beta}{2m_b^2 r} \right] \mathbf{L} \cdot \mathbf{S} \\ & + \left[\frac{\alpha_s}{3m_b^2 r^3} + \frac{\varepsilon\beta}{12m_b^2 r} \right] \mathbf{T}, \end{aligned} \quad (2)$$

where \mathbf{L} is the orbital momentum and \mathbf{S} is the spin of bottomonium. The singularity of contact hyperfine interaction within the spin-spin term has been smeared by Gaussian as $\tilde{\delta}_\sigma(r) = (\sigma/\sqrt{\pi})^3 e^{-\sigma^2 r^2}$ [21]. The involved operators are diagonal in a $|\mathbf{J}, \mathbf{L}, \mathbf{S}\rangle$ basis with the matrix elements,

$$\langle \mathbf{S}_b \cdot \mathbf{S}_{\bar{b}} \rangle = \frac{1}{2}S(S+1) - \frac{3}{4}, \quad (3)$$

$$\langle \mathbf{L} \cdot \mathbf{S} \rangle = \frac{1}{2}[J(J+1) - L(L+1) - S(S+1)], \quad (4)$$

$$\begin{aligned} \langle \mathbf{T} \rangle &= \left\langle \left[\frac{3}{r^2}(\mathbf{S}_b \cdot \mathbf{r})(\mathbf{S}_{\bar{b}} \cdot \mathbf{r}) - (\mathbf{S}_b \cdot \mathbf{S}_{\bar{b}}) \right] \right\rangle \\ &= -\frac{6(\langle \mathbf{L} \cdot \mathbf{S} \rangle)^2 + 3\langle \mathbf{L} \cdot \mathbf{S} \rangle - 2S(S+1)L(L+1)}{6(2L-1)(2L+3)}. \end{aligned} \quad (5)$$

Instead of separating the spin-dependent interactions into leading order parts, we solved the Schrödinger

equation of the unperturbed Hamiltonian with complete $V_{b\bar{b}}(r)$ including the spin-independent interactions as well as the spin-dependent terms,

$$\left[-\frac{\hbar^2}{2\mu_R}\nabla^2 + V_{b\bar{b}}(r) - E \right] \psi(\mathbf{r}) = 0, \quad (6)$$

where $\mu_R = m_b/2$ is the reduced mass. The interaction Hamiltonian including the kinetic and potential fully enables us to maintain the subtleness of the wave function. With the help of a well-chosen set of Gaussian basis functions, namely the Gaussian Expansion Method [24], the singular behavior of $1/r^3$ in spin-dependent terms at short distance can be refined variationally. The wave functions $\psi_{lm}(\mathbf{r})$ are expanded in terms of a set of Gaussian basis functions as

$$\psi_{lm}(\mathbf{r}) = \sum_{n=1}^{n_{max}} C_{nl} \left(\frac{2^{2l+\frac{7}{2}} \nu_n^{l+\frac{3}{2}}}{\sqrt{\pi}(2l+1)!!} \right)^{\frac{1}{2}} r^l e^{-(r/r_n)^2} Y_{lm}(\hat{\mathbf{r}}), \quad (7)$$

$$\nu_n = \frac{1}{r_n^2}, \quad r_n = r_1 a^{n-1}. \quad (8)$$

The dimension of Gaussian basis n_{max} is decided by variational principle. Considering the stableness of the eigen system, we set the basis-related parameters as $n_{max} = 9$, $r_1 = 0.1$ fm, $r_{n_{max}} = 2.2$ fm. In the Gaussian basis space, solving Eq.(6) involves the generalized eigenvalue problem. The analytic formulas of matrix elements with the Gaussian basis can be found in our previous work [23].

The five model-involved parameters are determined via fitting with the reasonably well-established $b\bar{b}$ states by minimizing the merit function

$$\chi^2 = \sum_{i=1}^N \left[\frac{M_i^{exp} - M_i^{th}(\mathbf{a})}{\sigma_i} \right]^2, \quad (9)$$

where N denotes the number of fitting data, the M_i^{th} indicates the theoretical value, the M_i^{exp} and σ_i are the experimental data and the associated errors. Given a trial set of model-dependent parameters \mathbf{a} , a procedure calculating the $\chi^2(\mathbf{a})$ is developed to improve the trial solution with the increments $\delta\mathbf{a}$ and repeated until $\chi^2(\mathbf{a}+\delta\mathbf{a})$ effectively stops decreasing. The obtained parameters are $m_b = 4.7935$ GeV, $\alpha_s = 0.3897$, $\beta = 0.1684$ GeV², $\sigma = 2.1054$ GeV and $\varepsilon = -0.1851$. The fitted value of ε implies that the vector exchange component is approximately one-fifth, which is close to one obtained for the charmonium system [23] and consistent with the result of Ref. [22].

3 Numerical results

3.1 Mass spectrum

Given the set of parameters, we predict the masses of the forty two $b\bar{b}$ states shown in Table 1, where we compare the present theoretical predictions with those from

the relativized extension of the nonrelativistic model [25] and a semirelativistic Hamiltonian under nonperturbative framework [22]. Fig. 1 illustrates the newly

found conventional $b\bar{b}$ states, i.e. $\eta_b(1S)$, $\eta_b(2S)$, $h_b(1P)$, $h_b(2P)$, $\Upsilon(1^3D_2)$ and the bottomonium-like $\Upsilon(10860)$ as well as the mass barycenter of the $\chi_b(3P)$.

Table 1. The experimental and theoretical bottomonium mass spectrums. The labeled states are used in the determination of potential parameters. We list the world average masses from PDG[26] as well as the latest observations[2, 3].

State	Expt. [26] [MeV]	Ref. [25] [GeV]	Ref. [22] [MeV]	Our [MeV]
$\eta_b(1^1S_0)$	9390.9 ± 2.8	9.40	9421.02	9409.17
$\Upsilon(1^3S_1)^*$	9460.3 ± 0.26	9.46	9460.28	9458.66
$\eta_b(2^1S_0)$	$9974.6 \pm 2.3 \pm 2.1[2]$	9.98	10003.6	9996.42
$\Upsilon(2^3S_1)^*$	10023.26 ± 0.31	10.00	10023.5	10012.1
$\eta_b(3^1S_0)$		10.34	10360.4	10334.9
$\Upsilon(3^3S_1)^*$	10355.2 ± 0.5	10.35	10365.6	10345.5
$\eta_b(4^1S_0)$			10631.5	10612.8
$\Upsilon(4^3S_1)$	10579.4 ± 1.2	10.63	10643.4	10623.3
$\eta_b(5^1S_0)$				10865.3
$\Upsilon(5^3S_1)$		10.88		10870.6
$\chi_{b2}(1^3P_2)^*$	9912.21 ± 0.26	9.90	9910.13	9924.98
$\chi_{b1}(1^3P_1)^*$	9892.78 ± 0.26	9.88	9892.83	9906.92
$\chi_{b0}(1^3P_0)^*$	9859.44 ± 0.42	9.85	9860.43	9858.59
$h_b(1^1P_1)$	$9898.3 \pm 1.1^{+1.0}_{-1.1}[3]$	9.88	9899.94	9911.97
$\chi_{b2}(2^3P_2)^*$	10268.65 ± 0.22	10.26	10271.1	10265.6
$\chi_{b1}(2^3P_1)^*$	10255.46 ± 0.22	10.25	10257.6	10250.1
$\chi_{b0}(2^3P_0)^*$	10232.5 ± 0.4	10.23	10231.4	10209.9
$h_b(2^1P_1)$	$10259.8 \pm 0.6^{+1.4}_{-1.0}[3]$	10.25	10263.1	10254.1
$\chi_{b2}(3^3P_2)$				10541.4
$\chi_{b1}(3^3P_1)$				10527.6
$\chi_{b0}(3^3P_0)$				10491.3
$h_b(3^1P_1)$				10531.2
$\chi_{b2}(4^3P_2)$				10839.9
$\chi_{b1}(4^3P_1)$				10814.9
$\chi_{b0}(4^3P_0)$				10755.2
$h_b(4^1P_1)$				10814.9
$\Upsilon(1^3D_3)$		10.16	10164.1	10155.9
$\Upsilon(1^3D_2)$	10163.7 ± 1.4	10.15	10157.0	10154.4
$\Upsilon(1^3D_1)$		10.14	10148.8	10149.6
1^1D_2		10.15	10158.3	10154.2
$\Upsilon(2^3D_3)$		10.45	10457.5	10441.5
$\Upsilon(2^3D_2)$		10.45	10451.2	10439.1
$\Upsilon(2^3D_1)$		10.44	10443.7	10433.7
2^1D_2		10.45	10452.4	10439.1
1^3F_4		10.36	10359.7	10337.3
1^3F_3		10.35	10355.6	10340.1
1^3F_2		10.35	10351.0	10340.8
1^1F_3		10.35	10355.9	10339.1
2^3F_4			10617.3	10597.3
2^3F_3			10613.4	10598.9
2^3F_2			10609.0	10598.6
2^1F_3			10613.7	10598.2

From the mass spectrum (Table 1 and Fig. 1), it can be seen that our predictions are in agreement with the experimental data reasonably. Regarding the $\Upsilon(4S)$,

unfortunately, all the three listed theoretical predictions are about 50 MeV higher than the observation. Since the $\Upsilon(4S)$ is quite close to the $B\bar{B}$ threshold, it

is reasonably shifted towards lower mass by the meson loops [27, 28]. The threshold effect would make sense on account of $\Upsilon(4S)$ or $\Upsilon(10580)$. $\Upsilon(10860)$ observed by Belle Collaboration [5, 6] has the world average mass $M = 10.876 \pm 0.011$ GeV and the full width $\Gamma = 55 \pm 28$ MeV [26]. Its structure has been investigated as the bottomonium 5^3S_1 state [10] and b -flavored $Y(4260)$ [5, 6]. In our prediction, the theoretical mass $\Upsilon(5S) M(5^3S_1) = 10870.61$ MeV is very close to the average value. However, the bottomonium interpretation of $\Upsilon(10860)$ will be challenged by the distinguishing partial widths for dipion transitions [6]. The radial excitation of the P -wave χ_b system was observed in the radiative tran-

sitions to $\Upsilon(1S)$ and $\Upsilon(2S)$ by the ATLAS Collaboration [4]. The mass barycenter of a spin-triplet was reported as $10.530 \pm 0.005 \pm 0.009$ GeV. Our theoretical prediction is $\bar{m}_3 \equiv [m(\chi_{b0}) + 3m(\chi_{b1}) + 5m(\chi_{b2})]/9 = 10.5313$ GeV, which coincides with the experimental data quite well. The bottomonium ground state $\eta_b(1S)$ was detected by BABAR Collaboration [29] and confirmed in other experiments. The world average mass of $\eta_b(1S)$ is $M = 9390.9 \pm 2.8$ MeV and it corresponds to the $\Upsilon(1S)$ hyperfine split $\Delta M_{HF}(1S) = 69.3 \pm 2.8$ MeV [26]. In the present theoretical framework, we predict $M_{th} = 9409.17$ MeV and $\Delta M_{HF}(1S) \approx 50$ MeV.

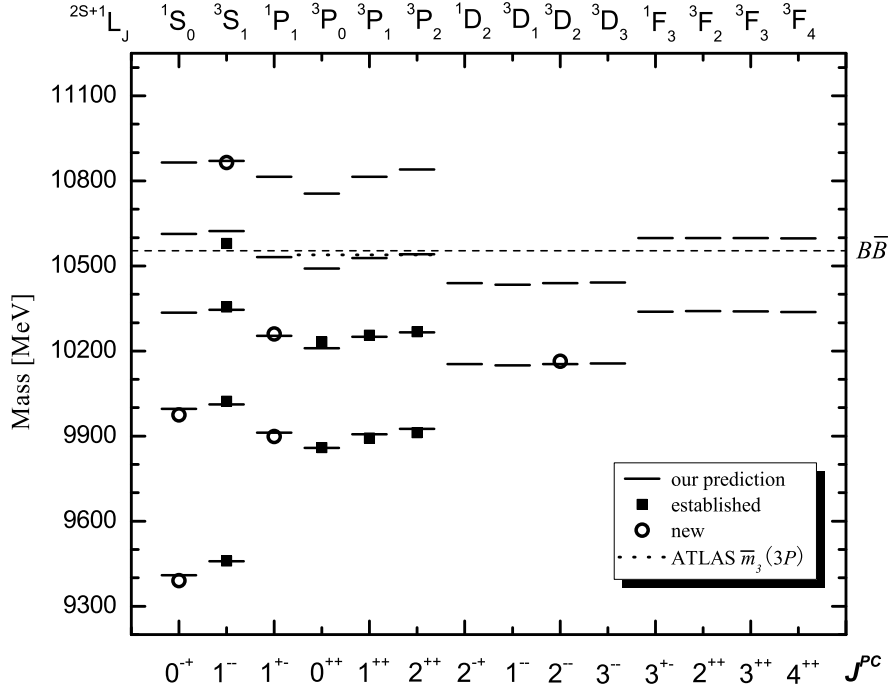


Fig. 1. The established and predicted mass spectrum of the bottomonium states.

3.2 Leptonic decays

The lowest-order expressions of electric decay width with the first-order QCD corrections [30] are

$$\Gamma_{ee}(nS) = \frac{4\alpha^2 e_b^2}{M_{nS}^2} |R_{nS}(0)|^2 \left(1 - \frac{16}{3} \frac{\alpha_s(m_b)}{\pi}\right), \quad (10)$$

$$\Gamma_{ee}(nD) = \frac{25\alpha^2 e_b^2}{2M_{nS}^2 m_b^4} |R''_{nD}(0)|^2 \left(1 - \frac{16}{3} \frac{\alpha_s(m_b)}{\pi}\right), \quad (11)$$

where e_b is the b -quark charge in units of $|e|$, $\alpha = 1/137.036$ is the fine-structure constant, M_{nS} and M_{nD} are the $(n_r+1)th$ S -wave and D -wave state mass respectively with the radial excitation number n_r . Note that here $\alpha_s(m_b)$ within potential are essentially the strong coupling constants but of different mass scales. We adopt $\alpha_s(m_b) = 0.18$ as in Refs. [9, 31]. $R_{nS}(0)$ is the radial S wave function at the origin, and $R''_{nD}(0)$ is the second derivative of the radial D -wave function at the origin. They are explicitly analytic in the Gaussian basis space [23]. Table 2 presents the numerical results.

Table 2. The leptonic decay width, in units of keV.

State	Ref. [9]		Ref. [32]	Ref. [33]	Our		Expt. [26]
	Γ_{ee}^0	Γ_{ee}			Γ_{ee}^0	Γ_{ee}	
$\Upsilon(1^3S_1)$	2.31	1.60	1.314	1.320	1.738	1.207	1.340 ± 0.018
$\Upsilon(2^3S_1)$	0.92	0.64	0.576	0.628	0.666	0.462	0.612 ± 0.011
$\Upsilon(3^3S_1)$	0.64	0.44	0.476	0.263	0.494	0.343	0.443 ± 0.08
$\Upsilon(4^3S_1)$	0.51	0.35	0.248	0.104	0.544	0.378	0.272 ± 0.029
$\Upsilon(5^3S_1)$	0.42	0.29	0.310	0.04	0.272	0.189	
$\Upsilon(1^3D_1)$					0.00121	0.000838	
$\Upsilon(2^3D_1)$					0.00205	0.00143	

3.3 Radiative transition

Because radiative transition is sensitively dependent on the detailed features of state wave functions, it is of great interest as a plausible inspection of meson structure. The transition rate between an initial bottomonium state i of radial quantum number n_i , orbital angular momentum L_i , spin S_i , and total angular momentum J_i , and a final state f with corresponding labels ($\hbar = c = 1$) is given in Ref. [34] as

$$\Gamma_{E1} \left(n_i^{2S_i+1} L_{iJ_i} \rightarrow n_f^{2S_f+1} L_{fJ_f} \right) = \frac{4}{3} C_{fi} \delta_{S_i S_f} e_b^2 \alpha \times |\langle \psi_f | r | \psi_i \rangle|^2 E_\gamma^3 \frac{E_f^{(b\bar{b})}}{M_i^{(b\bar{b})}}, \quad (12)$$

$$\Gamma_{M1} \left(n_i^{2S_i+1} L_{iJ_i} \rightarrow n_f^{2S_f+1} L_{fJ_f} \right) = \frac{4}{3} \frac{2J_f+1}{2L_i+1} e_b^2 \times \frac{\alpha}{m_b^2} \delta_{L_i L_f} \delta_{S_i, S_f \pm 1} |\langle \psi_f | \psi_i \rangle|^2 E_\gamma^3 \frac{E_f^{(b\bar{b})}}{M_i^{(b\bar{b})}}. \quad (13)$$

In the above formulas, e_b is the charge of b-quark in units of $|e|$, and M_i , E_f symbolize the eigen mass of initial $b\bar{b}$ and the total energy of final state respectively. The momentum of the final photon equals $E_\gamma = (M_i^2 - M_f^2)/(2M_i)$ to leading nonrelativistic order [35]. The variationally Gaussian expanded wave functions give rise to the analytic formulas for the overlap integral and the transition matrix elements[23]. The angular matrix element C_{fi} is

$$C_{fi} = \max(L_i, L_f)(2J_f+1) \begin{Bmatrix} L_f & J_f & S \\ J_i & L_i & 1 \end{Bmatrix}^2. \quad (14)$$

The numerical results of $E1$ and $M1$ transitions are presented in Tables 3-4 and 5, respectively. Our results are compatible with the observations for most channels.

Table 3. E1 radiative transitions

Initial	Final	E_γ [MeV]			Γ_{E1} [keV]			Expt.[26][keV]
		Ref. [34]	Ref. [9]	Our	Ref. [34]	Ref. [9]	Our	
$\Upsilon(2^3S_1)$	$\chi_{b2}(1^3P_2)$	110	110	110	2.14	2.62	2.64	2.287 ± 0.112
	$\chi_{b1}(1^3P_1)$	131	130	130	2.18	2.54	2.29	2.207 ± 0.128
	$\chi_{b0}(1^3P_0)$	162	163	162	1.39	1.67	1.047	1.215 ± 0.128
$\eta_b(2^1S_0)$	$h_b(1^1P_1)$		83	84		6.10	2.045	
$\Upsilon(3^3S_1)$	$\chi_{b2}(1^3P_2)$	433	434	434	0.025	0.25	0.681	< 0.386
	$\chi_{b1}(1^3P_1)$	453	452	452	0.017	0.17	0.0886	< 0.0345
	$\chi_{b0}(1^3P_0)$	484	484	484	0.007	0.007	0.0495	0.0610 ± 0.0224
$\eta_b(3^1S_0)$	$h_b(1^1P_1)$		418	414		1.24	0.997	
$\Upsilon(3^3S_1)$	$\chi_{b2}(2^3P_2)$	86		86	2.78		3.138	2.662 ± 0.325
	$\chi_{b1}(2^3P_1)$	99		99	2.52		2.538	2.561 ± 0.244
	$\chi_{b0}(2^3P_0)$	124		122	1.65		1.122	1.200 ± 0.122
$\eta_b(3^1S_0)$	$h_b(2^1P_1)$			80	2.14		4.471	
$\chi_{b2}(1^3P_2)$	$\Upsilon(1^3S_1)$	443	442	455	37.8	38.2	35.739	
$\chi_{b1}(1^3P_1)$		443	423	438	32.8	33.6	33.310	
$\chi_{b0}(1^3P_0)$		392	391	392	26.1	26.6	25.376	
$h_b(1^1P_1)$	$\eta_b(1^1S_0)$		501	490		55.8	39.015	
$\chi_{b2}(2^3P_2)$	$\Upsilon(2^3S_1)$	242	243	250	18.7	18.8	17.326	
$\chi_{b1}(2^3P_1)$		230	230	235	15.9	15.9	16.505	

Table 4. E1 radiative transitions (continued)

Initial	Final	E_γ [MeV]			Γ_{E1} [keV]			Expt. [26][keV]
		Ref. [34]	Ref. [9]	Our	Ref. [34]	Ref. [9]	Our	
$\chi_{b0}(2^3P_0)$		205	207	196	11.3	11.7	12.092	
$h_b(2^1P_1)$	$\eta_b(2^1S_0)$		266	254		24.7	17.61	
$\chi_{b2}(2^3P_2)$	$\Upsilon(1^3S_1)$	777	777	775	9.75	12.0	13.736	
$\chi_{b1}(2^3P_1)$		765	764	761	9.31	12.4	9.618	
$\chi_{b0}(2^3P_0)$		742	743	724	8.48	11.4	2.354	
$h_b(2^1P_1)$	$\eta_b(1^1S_0)$		831	810		15.9	14.861	
$\chi_{b2}(2^3P_2)$	$\Upsilon(1^3D_3)$	107	113	109	2.62	3.33	2.781	
	$\Upsilon(1^3D_2)$	112	117	111	0.54	0.66	0.488	
	$\Upsilon(1^3D_1)$	119	123	115	0.043	0.05	0.0342	
$\chi_{b1}(2^3P_1)$	$\Upsilon(1^3D_2)$	99	104	95	1.86	2.21	1.755	
	$\Upsilon(1^3D_1)$	106	110	100	0.76	0.92	0.631	
$\chi_{b0}(2^3P_0)$	$\Upsilon(1^3D_1)$	81	87	60	1.36	1.83	0.682	
$h_b(2^1P_1)$	$h_{b2}(1^1D_2)$		104	99		7.74	2.603	
$\chi_{b2}(3^3P_2)$	$\Upsilon(3^3S_1)$	170	183	194	12.1	15.6	16.250	
$\chi_{b1}(3^3P_1)$		159	167	181	10.1	12.0	15.270	
$\chi_{b0}(3^3P_0)$		144	146	145	7.46	7.88	10.331	
$h_b(3^1P_1)$	$\eta_b(3^1S_0)$		196	194		19.2	16.286	
$\chi_{b2}(3^3P_2)$	$\Upsilon(2^3S_1)$	491	504	516	3.78	6.00	5.923	
$\chi_{b1}(3^3P_1)$		481	489	503	3.56	5.48	4.192	
$\chi_{b0}(3^3P_0)$		466	468	468	3.24	4.80	0.762	
$h_b(3^1P_1)$	$\eta_b(2^1S_0)$		528	521		6.89	5.828	
$\chi_{b2}(3^3P_2)$	$\Upsilon(1^3S_1)$	1012	1024	1027	3.80	7.09	7.330	
$\chi_{b1}(3^3P_1)$		1003	1010	1015	3.69	6.80	4.238	
$\chi_{b0}(3^3P_0)$		989	990	982	3.54	6.41	0.217	
$h_b(3^1P_1)$	$\eta_b(1^1S_0)$		1078	1062		8.27	7.668	
$\chi_{b2}(3^3P_2)$	$\Upsilon(2^3D_3)$	82	97	99	3.01	5.05	4.662	
	$\Upsilon(2^3D_2)$	85	101	102	0.61	1.02	0.841	
	$\Upsilon(2^3D_1)$	91	107	107	0.05	0.08	0.0603	
$\chi_{b1}(3^3P_1)$	$\Upsilon(2^3D_2)$	75	86	88	2.08	3.10	3.098	
	$\Upsilon(2^3D_1)$	81	92	94	0.86	1.26	1.146	
$\chi_{b0}(3^3P_0)$	$\Upsilon(2^3D_1)$			57			1.348	
$h_b(3^1P_1)$	$h_{b2}(2^1D_2)$			92			4.537	
$\chi_{b2}(3^3P_2)$	$\Upsilon(1^3D_3)$		377	379	≈ 0	≈ 0	0.000261	
	$\Upsilon(1^3D_2)$		381	379	≈ 0	≈ 0	0.000786	
	$\Upsilon(1^3D_1)$		387	385	≈ 0	≈ 0	0.003803	
$\chi_{b1}(3^3P_1)$	$\Upsilon(1^3D_2)$		366	367	≈ 0	≈ 0	0.0584	
	$\Upsilon(1^3D_1)$		372	371	≈ 0	≈ 0	0.00479	
$\chi_{b0}(3^3P_0)$	$\Upsilon(1^3D_1)$		336	336	≈ 0	≈ 0	0.957	
$h_b(3^1P_1)$	$h_{b2}(1^1D_2)$		370	370	≈ 0	≈ 0	0.0384	
$\Upsilon(1^3D_3)$	$\chi_{b2}(1^3P_2)$	245	240	228	24.3	26.4	22.060	
$\Upsilon(1^3D_2)$	$\chi_{b2}(1^3P_2)$	240	236	227	5.7	6.29	5.438	
	$\chi_{b2}(1^3P_1)$	261	255	245	22.0	23.8	18.481	
$\Upsilon(1^3D_1)$	$\chi_{b2}(1^3P_2)$	233	230	222	0.58	0.65	0.570	
$\Upsilon(1^3D_1)$	$\chi_{b2}(1^3P_1)$	254	249	240	11.3	12.3	9.765	
	$\chi_{b2}(1^3P_0)$	285	282	287	21.4	23.6	17.267	
$h_{b2}(1^1D_2)$	$h_b(1^1P_1)$		246	239		42.3	23.780	
$\Upsilon(2^3D_3)$	$\chi_{b2}(1^3P_2)$	518	517	504	3.94	4.01	3.042	
$\Upsilon(2^3D_2)$	$\chi_{b2}(1^3P_2)$	514	513	501	0.97	0.98	0.551	
	$\chi_{b2}(1^3P_1)$	534	531	519	3.25	3.26	3.285	
$\Upsilon(2^3D_1)$	$\chi_{b2}(1^3P_2)$	509	507	496	0.10	0.11	0.0353	
	$\chi_{b2}(1^3P_1)$	529	525	513	1.75	1.76	1.266	
	$\chi_{b2}(1^3P_0)$	559	557	559	2.76	2.79	5.208	
$h_{b2}(2^1D_2)$	$h_b(1^1P_1)$		522	514		6.19	3.853	

Table 5. M1 radiative partial widths

Initial	Final	E_γ [MeV]	Γ_{M1} [keV]	Expt. [26] [keV]
$\Upsilon(1^3S_1)$	$\eta_b(1^1S_0)$	49	5.605	
$\Upsilon(2^3S_1)$	$\eta_b(2^1S_0)$	16	0.180	
	$\eta_b(1^1S_0)$	585	19.933	12.47 ± 4.80
$\eta_b(2^1S_0)$	$\Upsilon(1^3S_1)$	523	46.385	
$\Upsilon(3^3S_1)$	$\eta_b(3^1S_0)$	11	0.0556	
	$\eta_b(2^1S_0)$	343	2.515	< 12.60
	$\eta_b(1^1S_0)$	894	19.029	10.36 ± 1.42
$\eta_b(3^1S_0)$	$\Upsilon(2^3S_1)$	318	6.806	
	$\Upsilon(1^3S_1)$	839	45.005	
$h_b(2^1P_1)$	$\chi_{b2}(1^3P_2)$	324	3.806	
	$\chi_{b1}(1^3P_1)$	341	0.449	
	$\chi_{b0}(1^3P_0)$	388	14.062	
$\chi_{b2}(2^3P_2)$	$h_b(1^1P_1)$	347	2.566	
$\chi_{b1}(2^3P_1)$	$h_b(1^1P_1)$	333	0.431	
$\chi_{b0}(2^3P_0)$	$h_b(1^1P_1)$	294	25.509	
$h_b(3^1P_1)$	$\chi_{b2}(2^3P_2)$	262	2.653	
	$\chi_{b1}(2^3P_1)$	277	0.277	
	$\chi_{b0}(2^3P_0)$	316	8.604	
	$\chi_{b2}(1^3P_2)$	589	5.286	
	$\chi_{b1}(1^3P_1)$	606	0.600	
	$\chi_{b0}(1^3P_0)$	651	19.314	
$\chi_{b2}(3^3P_2)$	$h_b(2^1P_1)$	283	1.745	
	$h_b(1^1P_1)$	611	3.578	
$\chi_{b1}(3^3P_1)$	$h_b(2^1P_1)$	270	0.271	
	$h_b(1^1P_1)$	598	0.572	
$\chi_{b0}(3^3P_0)$	$h_b(2^1P_1)$	235	17.450	
	$h_b(1^1P_1)$	563	35.015	

4 Summary

The bottomonium mass spectrum, electromagnetic transitions and leptonic widths are investigated by adopting the quark-antiquark potential consisting of the one-gluon-exchange and the Lorentz scalar-vector mixing linear confining potentials. We perform a nonperturbative calculation to the full Hamiltonian including spin-independent and -dependent potentials. Fitting with the mass of the ten well-established $b\bar{b}$ states, the vector scale parameter ε is determined and implies the 18.51% vector component of confining interaction. Combining our previous work on charmonium systems[23], we found that the scalar-vector mixing linear confinement of heavy quarkonium seems to be important and nearly about one-fifth; explicitly, it is slightly lower than 4% for the bottomonium mesons.

In our calculation, the mass spectrum accords reasonably well with the newly observed family members of bottomonium, i.e. $\eta_b(1S)$, $\eta_b(2S)$, $h_b(1P)$, $h_b(2P)$, $\Upsilon(1^3D_2)$ and the $\chi_b(3P)$ structure. The mass and leptonic decay width of 5^3S_1 is very close to the data of the bottomonium-like $\Upsilon(10860)$ released by Belle in our calculation and Ref [32], respectively. However, the bottomonium interpretation of $\Upsilon(10860)$ will be challenged

by the distinguishing partial widths for dipion transitions [6]. Very recently, the production rates have been calculated by Ahmed and Wang [36] for the processes $pp(\bar{p}) \rightarrow Y_b(10890)(\rightarrow \Upsilon(1S, 2S, 3S)\pi^+\pi^- \rightarrow \mu^+\mu^-\pi^+\pi^-)$, by taking the $Y_b(10890)$ as a tetraquark state. Further experiment at the LHC and the Tevatron will help us to understand its structure. The corresponding $E1$, $M1$ radiative transitions and leptonic decay widths have been theoretically predicted for the further experimental search and enrichment of the bottomonium family.

References

- Eidelman S et al. arXiv:hep-ex/1205.4189.
- Dobbs S et al. Phys. Rev. Lett., 2012, **109**: 082001 [arXiv:hep-ex/1204.4205v1]
- Adachi I et al.(Belle Collaboration). Phys. Rev. Lett., 2012, **108**: 03200 [arXiv:hep-ex/1103.3419]
- Aad G et al.(ATLAS Collaboration). Phys. Rev. Lett. 2012, **108**: 152001 [arXiv:hep-ex/1112.5154]
- Chen K F et al.(Belle Collaboration). Phys. Rev. Lett., 2008, **100**: 112001
- Chen K F et al.(Belle Collaboration). Phys. Rev. D, 2010, **82**: 091106
- Lovelock D et al. Phys. Rev. Lett., 1985, **54**: 377
- Besson D et al.(CLEO Collaboration). Phys.Rev.Lett., 1985, **54**: 381
- Li B Q and Chao K T. Commun. Theor. Phys., 2009, **52**: 653[arXiv:hep-ph/0909.1369]

- 10 Hou W S. Phys. Rev. D, 2006, **74**: 017504
- 11 Eichten E et al. Phys. Rev. Lett., 1976, **36**: 500
- 12 Brambilla N et al.(Quarkonium Working Group). Eur. Phys. J. C, 2011, **71**: 1534 [arXiv:hep-ph/1010.5827v3]
- 13 Eichten E et al. Phys. Rev. D, 1978, **17**: 3090
- 14 Shizuya K and Tye S H H. Phys. Rev. D, 1980, **21**: 313
- 15 Buchmuller W. Phys. Lett. B, 1982, **112**: 479
- 16 Ebert D, Faustov R N and Galkin V O. Phys. Rev. D, 2003, **67**: 014027
- 17 Ebert D, Faustov R N and Galkin V O. Phys. Rev. D, 2000, **67**: 034014
- 18 McClary R and Byers N. Phys. Rev. D, 1983, **28**: 1692
- 19 Galkin V O and Faustov R N. Yad. Fiz., 1986, **44**: 1575 [Sov. J. Nucl. Phys., 1986, **44**: 1023]
- 20 Galkin V O, Mishurov A Y and Faustov R N. Yad. Fiz., 1990, **51**:1101 [Sov. J. Nucl. Phys., 1992, **51**: 1027]
- 21 Barnes N, Godfrey S and Swanson E S. Phys. Rev. D, 2005, **72**: 054026
- 22 Radford S F and Repko W W. Phys. Rev. D, 2007, **75**: 074031
- 23 Cao L, Yang Y C and Chen H. Few-Boby Syst, 2012, **53**: 327 [arXiv:hep-ph/1206.3008]
- 24 Hiyama E, Kino Y and Kamimura M. Prog, Part. Nucl. Phys., 2003, **51**: 223
- 25 Godfrey S and Isgur N. Phys. Rev. D, 1985, **32**: 189
- 26 Beringer J et al.(Particle Data Group). Phys. Rev. D, 2012, **86**: 1223
- 27 van Beveren E and Rupp G. Phys. Rev. D, 2009, **80**: 074001
- 28 van Beveren E and Rupp G. arXiv:hep-ph/1010.1401
- 29 Aubert B et al.(BABAR Collaboration). Phys. Rev. Lett., 2008, **101**: 071801
- 30 Kwong W et al. Phys. Rev. D, 1988, **37**: 3210
- 31 Ebert D, Faustov R N and Galkin V O. Mod. Phys. Lett. A, 2003, **18**: 601 [arXiv:hep-ph/0302044]
- 32 Anisovich V V, Dakhno L G, Matveev M A et al. Phys. Atom. Nucl., 2007, **70**: 63 [arXiv:hep-ph/0510410]
- 33 Pandya J N, Rai A K and Vinodkumar P C. Frascati Phys. Ser, 2007, **46**: 1519 [arXiv:hep-ph/0808.1077v1]
- 34 Kwong W and Rosner J L. Phys. Rev. D, 1988, **38**: 279
- 35 Brambilla N, Krämer M, Mussa R et al. arXiv:hep-ph/0412158
- 36 Ali Ahmed and Wang Wei. Phys. Rev. Lett., 2011, **106**: 192001